CMOS-Foundry Compatible, Broadband, and Compact Routing of Multimode SOI Waveguides

Asher Novick,[1,*] Kaylx Jang,[1] Anthony Rizzo,[1] Aneek James,[1] Utsav Dave,[1] Michal Lipson,[1] and Keren Bergman[1]

[1]*Department of Electrical Engineering, Columbia University, New York, NY, 10027, USA*

[*]*asher.novick@columbia.edu*

Abstract: We demonstrate a CMOS-foundry compatible, broadband, and compact platform for routing multimode wavguides. Insertion loss of <0.5dB and modal cross-talk of <-15dB are measured for 90° and 180° $R_{eff} < 3\mu$m bends supporting over 200nm of bandwidth.

1. Introduction

The bandwidth demands of data center and high performance computing systems necessitate the adoption of co-packaged optical interconnects in next-generation systems to keep pace with application requirements. Silicon photonics presents the most promising path for co-packaged optics due to its compatibility with standard complementary metal-oxide-semiconductor (CMOS) foundries used to fabricate microelectronic chips. While the high index contrast of the silicon-on-insulator (SOI) platform permits extreme device density on-chip, interfacing with the relatively large size of standard optical fiber presents a bottleneck to continued scaling. Therefore, multiplexing and routing parallel data streams on a single bus is critical to maximizing the achievable per-fiber bandwidth. In this direction, both wavelength-division multiplexing (WDM) [1] and mode-division multiplexing (MDM) [2, 3] have been explored as orthogonal axes of scaling. Solutions leveraging both WDM *and* MDM show the greatest promise in terms of achievable bandwidth density; thus, enabling on-chip routing of multiple modes across a broad wavelength bandwidth is key to enabling future-generation WDM-MDM interconnects. Previous demonstrations of multi-mode routing for MDM have relied on difficult-to-fabricate structures such as sub-wavelength features [4] and heterogeneously integrated non-CMOS-native materials [5].

Here, we propose and demonstrate a high-performance CMOS-compatible platform for routing multiple spatial modes across 200 nm of optical bandwidth with high channel isolation, cross-talk as low as -20 dB, and low insertion loss (IL) below 0.5 dB for waveguides supporting between 2 and 5 modes. Beyond preserving mode orthogonality for a wide range of wavelength and spatial mode channels, the platform is inherently robust to fabrication variations in the waveguide geometry, as described in [6]. We experimentally demonstrate our platform using devices fabricated in a commercial 300 mm CMOS foundry with state-of-the-art performance.

2. Multimode Waveguide Bend Model and Simulation Results

Multimode waveguides provide signficant gains in fabrication robustness for phase sensitive single mode applications, but this comes at the cost of supporting the propagation of more than one transverse electric (TE) mode. The effective index (n_{eff}) sensitivity of TE0 as a function of waveguide width is illustrated in Fig. 1a. Routing these waveguides via radial bends, as defined by $x^2+y^2=R^2$, introduces significant modal cross-talk, primarily due the sharp transition between the mode field profiles of a straight waveguide and a bent waveguide. To avoid this, we employ Euler bends, where the radius of curvature varies linearly along the path length as defined by the Fresnel integrals,

$$S(x) = \int_0^x \sin\left(\frac{t^2}{2R_0^2}\right) dt, \qquad C(x) = \int_0^x \cos\left(\frac{t^2}{2R_0^2}\right) dt, \tag{1}$$

where s is the normalized path length, R_0 is the parameter of the Euler curve, and the curvature function is $\kappa(s) = \frac{2s}{R_0^2}$. Due to the adiabatic transition between straight and bent waveguides, the propagating modes are not perturbed and can remain orthogonal, thus resulting in high modal isolation and transmission [6].

Due to its adiabatic nature, an Euler bend is longer in path length and reaches a reduced minimum radius of curvature (R_{min}) relative to the equivalent radial bend with radius R_{eff}. Fig. 1b shows a radial bend overlaid with several Euler bends for bend angles between 45° and 180^o. While the smooth transition between bend curvature supports mode orthogonality, certain R_{min} values can still result in mode perturbation. Fig. 1c illustrates the simulated broadband transmission of TE0 as a function of R_{eff} for a 220 nm x 1200 nm wide 90° Euler bend.

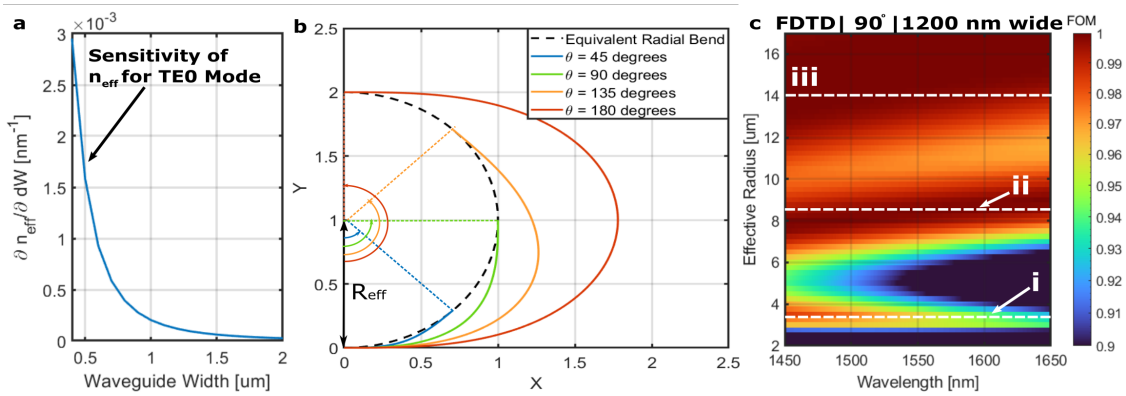

Fig. 1. **a)** Simulated n_{eff} sensitivity for TE0 to fabrication width variation as a function of target waveguide width. **b)** Euler bends starting at the origin, plotted for 45^o, 90^o, 135^o, and 180^o, relative to a radial bend of equivalent radius. Axes are normalized relative to R_{eff}. **c)** Simulated TE0⟶TE0 spectral transmission for a 220 nm x 1200 nm SOI waveguide around a 90° Euler bend. High transmission occurs in several regions, *i)* $R_{eff} \approx 3.25\,\mu$m, *ii)* $R_{eff} \approx 8.5\,\mu$m, *iii)* and $R_{eff} \geq 14\,\mu$m, indicating target R_{eff} design values for a 90° 1200 nm wide Euler bend.

3. Experimental Measurements

A variety of 90° and 180° Euler bends were fabricated for different waveguide widths (up to 2 μm, supporting TE0 through TE4) and R_{eff}s. Measurements were made using pairs of edge coupled adiabatic MDM structures to couple in and out of specific TE modes, as shown in Fig. 2a. Reference measurements with straight waveguides between MDM structures are used to de-embed the edge coupler and MDM performance from the bends.

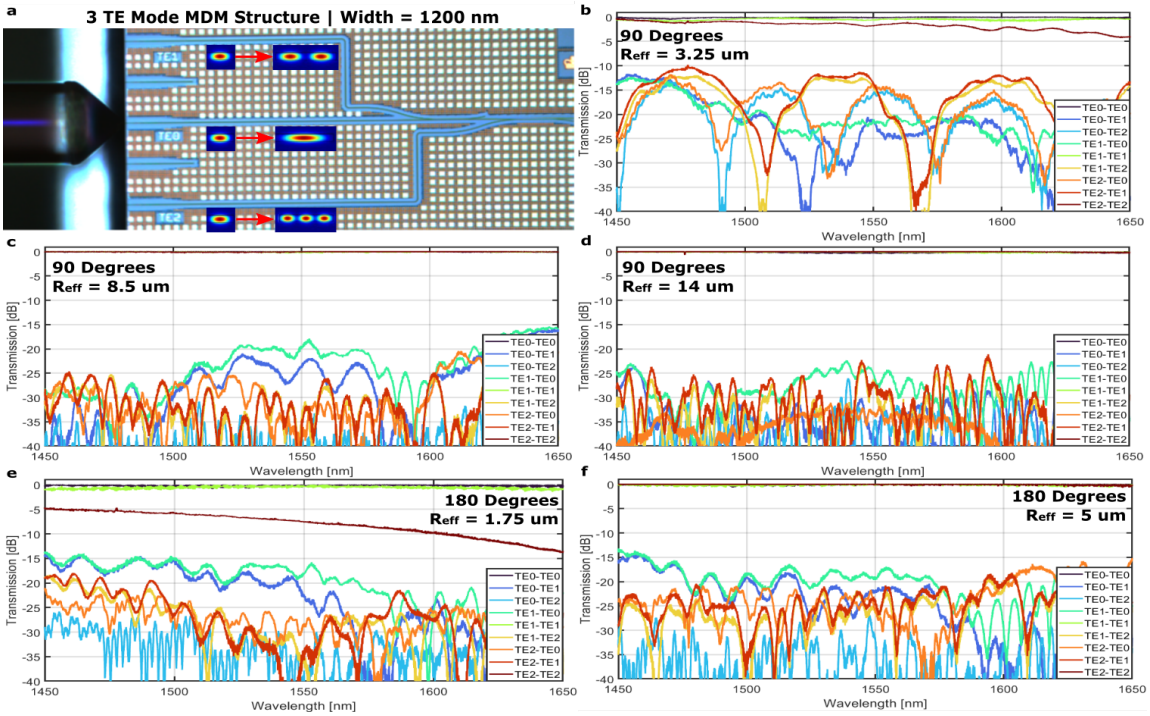

Fig. 2. **a)** Microscope image of experimental setup for 220 nm x 1200 nm wide waveguides (3 TE modes). Insets visualize the field profile of the mode that each edge coupler corresponds to. Measured per-bend modal-spectral transmission of the same waveguide's Euler bends, for 90° bends with **b)** $R_{eff} = 3.25\,\mu$m and modal crosstalk ≤ -10 dB, **c)** $R_{eff} = 8.5\,\mu$m and modal crosstalk ≤ -15 dB, **d)** $R_{eff} = 14\,\mu$m and modal crosstalk ≤ -20 dB, as well for 180° bends with **e)** $R_{eff} = 1.75\,\mu$m and modal crosstalk ≤ -15 dB, **f)** $R_{eff} = 5\,\mu$m with modal crosstalk ≤ -18 dB.

Fig. 2 shows the the modal transmission for three 90° and two 180° Euler bends for a 220 nm x 1200 nm waveguide. The measured three 90° bends are in good agreement with the three annotated simulation high transmission regions in Fig. 1c. 180° Euler bends similarly demonstrate the 3 regions of high performance. For the same R_{eff}, the R_{min} of a 180° bend is larger than for a 90° Euler bend. As a result, the 180° R_{eff} can be substantially reduced while maintaining high transmission and mode isolation. Fig. 2e shows $R_{eff} = 1.75\,\mu$m with < 0.5 dB loss for TE0 transmission and < 1 dB loss for TE1 transmission, though TE2 is significantly attenuated. Fig. 2f shows similar performance with an $R_{eff} = 5\,\mu$m as with Fig. 2c, negligible IL for all three modes and less than -15 dB modal cross-talk across nearly the full 200 nm of optical bandwidth is measured.

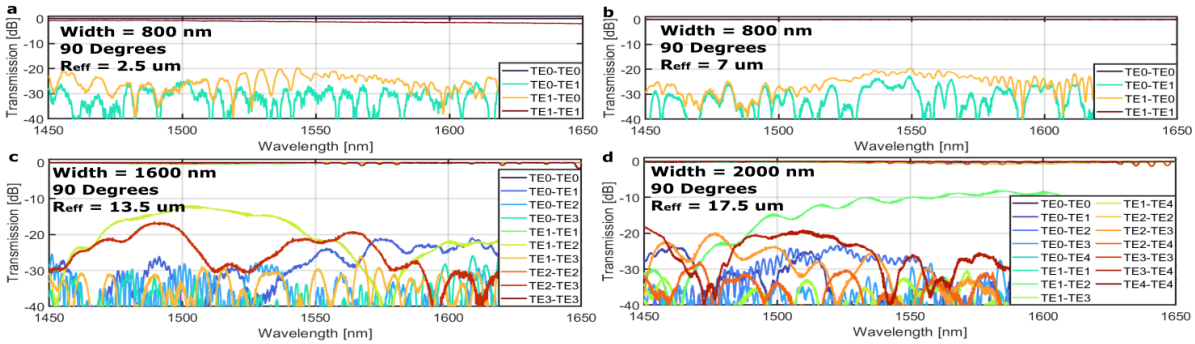

Fig. 3. Measured per-bend modal-spectral transmission of 220 nm x Width waveguide Euler bends, for 90° bends with **a)** Width = 800 nm, $R_{eff} = 2.5\,\mu$m, and modal crosstalk ≤ -20 dB, **b)** Width = 800 nm, $R_{eff} = 7\,\mu$m, and modal crosstalk ≤ -20 dB, **c)** Width = 1600 nm, $R_{eff} = 13.5\,\mu$m, and modal crosstalk ≤ -12 dB, and **d)** Width = 2000 nm, $R_{eff} = 17.5\,\mu$m, and modal crosstalk ≤ -10 dB.

Measured modal transmissions for 90° Euler bends with widths of 800 nm, 1600 nm, and 2000 nm are shown in Fig. 3a-d, demonstrating the general applicability of this routing platform for various orders of MDM across a broad bandwidth. Fig. 3a corresponds to the simulated region *i* from Fig. 1c but for Width = 800 nm, while Fig. 3b-d correspond to region *ii* from Fig. 1c for their respective waveguide widths and bend angles.

4. Conclusion

We demonstrate an inherently fabrication-robust, broadband, scalable, and compact platform for routing multimode SOI waveguides for both MDM and phase-sensitive single mode applications. For MDM applications, high modal transmission and low crosstalk are demonstrated up through TE4 (5 simultaneous modes). Additionally, for phase-sensitive single mode operation, where multimode waveguides are used with only TE0 for their reduced sensitivity to fabrication variation, a new regime (Fig. 1c, region *i*) for compactness is demonstrated in simulation and experimentally validated. The ultra-broadband performance and compact footprint of the demonstrated waveguide routing platform enables unprecedented on-chip bandwidth density in future silicon photonic interconnects leveraging simultaneous WDM and MDM.

References

1. A. Rizzo, S. Daudlin, A. Novick *et al.*, "Petabit-scale silicon photonic interconnects with integrated kerr frequency combs," IEEE J. Sel. Top. Quantum Electron. **29**, 1–20 (2022).
2. L.-W. Luo, N. Ophir, C. P. Chen, L. H. Gabrielli, C. B. Poitras, K. Bergman, and M. Lipson, "Wdm-compatible mode-division multiplexing on a silicon chip," Nat. communications **5**, 1–7 (2014).
3. C. Li, D. Liu, and D. Dai, "Multimode silicon photonics," Nanophotonics **8**, 227–247 (2019).
4. Y. Liu *et al.*, "Arbitrarily routed mode-division multiplexed photonic circuits for dense integration," Nat. communications **10**, 1–7 (2019).
5. H. Xu and Y. Shi, "Ultra-sharp multi-mode waveguide bending assisted with metamaterial-based mode converters," Laser & Photonics Rev. **12**, 1700240 (2018).
6. A. Rizzo, U. Dave, A. Novick, A. Freitas, S. P. Roberts, A. James, M. Lipson, and K. Bergman, "Fabrication-robust silicon photonic devices in standard sub-micron silicon-on-insulator processes," arXiv preprint arXiv:2205.11481 (2022).

Acknowledgements: This work was supported in part by the U.S. Defense Advanced Research Projects Agency under PIPES Grant HR00111920014 and in part by the U.S. Advanced Research Projects Agency–Energy under ENLITENED Grant DE-AR000843. The wafer/chip fabrication and custom device processing were provided by AIM Photonics/SUNY Poly Photonics engineering team and fabricator in Albany, New York.